HOKKAIDO UNIVERSITY

Title	Quantification of organic fluorophores in absorbing media by solid-phase fluorescence excitation-emission matrix (SPF-EEM) spectroscopy of modeled mixtures containing bovine serum albumin (BSA) and colorants
Author(s)	Nakaya, Yuki; Tomita, Ayaka; Ochiai, Kosuke et al.
Citation	Spectrochimica Acta Part A: Molecular and Biomolecular Spectroscopy, 285, 121885 https://doi.org/10.1016/j.saa.2022.121885
Issue Date	2023-01-15
Doc URL	https://hdl.handle.net/2115/92965
Rights	© <2023>. This manuscript version is made available under the CC-BY-NC-ND 4.0 license http://creativecommons.org/licenses/by-nc-nd/4.0/
Rights(URL)	https://creativecommons.org/licenses/by-nc-nd/4.0/
Type	journal article
File Information	Nakaya_et_al_SAA_2022_accepted_manuscript.pdf

Hokkaido University Collection of Scholarly and Academic Papers : HUSCAP

Quantification of organic fluorophores in absorbing media by solid-phase fluorescence excitation–emission matrix (SPF-EEM) spectroscopy of modeled mixtures containing bovine serum albumin (BSA) and colorants

Yuki Nakaya[1, *], *Ayaka Tomita*[2], *Kosuke Ochiai*[2], *Hiroshi Yamamura*[2]

[1] Division of Environmental Engineering, Faculty of Engineering, Hokkaido University, North-13, West-8, Kita-ku, Sapporo, 060-8628, Japan

[2] Faculty of Science and Engineering, Chuo University, 1-13-27 Kasuga, Bunkyo-ku, Tokyo 112-8551, Japan.

*Corresponding Author

Abstract

Solid-phase fluorescence excitation–emission matrix (SPF-EEM) spectroscopy is beneficial for investigating the characteristics of natural organic matter (NOM) in the solid phase without extraction procedures. However, inner filter effect (IFE) due to the presence of dark components in samples can make it difficult to quantify the fluorophore concentration. To establish a new method to determine unknown concentrations of a fluorescent material in a sample containing various absorbing materials by SPF spectroscopy, modeled mixtures containing bovine serum albumin (BSA) and colorants at different ratios were examined. Fluorescence intensities of BSA against various concentrations afforded different saturation curves for different colorants in the mixtures, suggesting that it is difficult to use the SPF intensity for quantifying the concentration of fluorescent samples in which IFE has occurred, because one cannot obtain a single calibration curve that does not depend on the absorbing medium that it is mixed in. However, products of the fluorescence intensity and Kubelka–Munk (KM) function at the excitation wavelength were proportional to the first order of BSA weight concentrations, regardless of the colorant type. By using this trend as a calibration curve, it may be possible to quantify the amount of BSA from its SPF-EEM spectrum. In this study, the KM function was obtained using an ultraviolet–visible (UV–Vis) spectrometer with an integrating sphere. To reduce the labor and equipment cost of UV–Vis spectroscopy, a substrate of the KM function also was obtained from the Rayleigh scattering in an SPF-EEM spectrum, which could be used as a parameter for calibration curves that quantify the BSA concentration. Although further studies are required, this study proposed that the product of the SPF intensity and KM function at the excitation wavelength can be partially used for an empirical formula to quantify a variety of fluorescent materials mechanically mixed with various absorbing materials.

Keywords

Solid-phase fluorescence spectroscopy; Natural organic matter; Inner filter effect; Diffuse reflection spectrum; Rayleigh scattering.

Introduction

Natural organic matter (NOM) plays a key role in environmental processes of soil and water [1]. NOM is also important in drinking-water treatment as it can cause various problems [2]; it is a precursor of chlorinated carbonaceous disinfection by-products (DPBs) [3], and it can be a source of organic fouling materials in membrane filtration [4], etc.

For the liquid-phase analysis of NOM, three-dimensional excitation–emission matrix (3D-EEM) fluorescence spectroscopy is one of the beneficial methods because it is simple, sensitive, and non-destructive for qualitative and quantitative purposes. On the other hand, the analysis of NOM in soil, sludge, membranes, and biofilms by fluorescence spectroscopy also may be required. The analysis of such solid samples needs to be conducted in the liquid phase by extraction.

Generally, the organic content extracted from soils, sediments, and natural water by using alkali solutions and/or resins is regarded as the fraction of "humic substances" [5,6]. However, these extraction operations are both time- and labor-intensive. Moreover, the validity of NOM alkali extraction has been debated recently because alkali treatment may cause laboratory artifacts [7,8,9,10]. Some components of membrane fouling organic materials have been reported to not be extracted completely [11]. In the analysis of extracellular polymeric substances (EPS) of activated sludge in wastewater treatment, artifacts and alterations caused by extraction with alkali and/or ethylenediaminetetraacetic acid (EDTA) should be considered [12]. Therefore, for the analysis of organic matter in nature and water treatment, a method for analyzing NOM that does not require extraction is required.

In this regard, laser-induced fluorescence spectroscopy has been applied to solid NOM samples without extraction procedures to investigate the transformation of organic matter in samples [13], after the pioneering study on soils reported by Milori et al. (2008) [14]. In the past decade, 3D-

63 EEM fluorescence spectroscopy also has been applied to fluorescent solid samples such as organic
64 wastes [15], pharmaceutical preparations [16], model mixtures simulating natural soils [17],
65 composts [18], humic substances [19], modeled pure chemicals (such as tryptophan and quinine
66 sulfate) [19], fouling materials adhered to a membrane filter [20,21,22,23], and natural soils [24].
67 SPF spectroscopy also has been reportedly applied to foods [25] and paintings [26,27].
68 On the other hand, inner filter effect (IFE) is one of the difficulties in fluorescence spectroscopy
69 because it can disrupt the proportional relationship between the amount of fluorescent species and
70 actual observed intensity of fluorescence. In SPF-EEM spectroscopy, IFE caused by the dark color
71 of organic and inorganic materials is an issue [15,17,19,21,24].
72 This extinction of fluorescence is generally caused by strongly absorbing materials that cause
73 self-absorption of excitation light, re-absorption of emitted light, and/or scattering of such light.
74 For liquid samples, a sample solution can be diluted to prevent IFE. Furthermore, the method
75 proposed by Lakowicz (1999) [28] for correcting the fluorescence intensity at certain excitation
76 and emission wavelengths by using a factor containing absorbance at those wavelengths also can
77 be applied. Various theoretical and empirical methods of fluorescence correction have been
78 proposed for LPF spectroscopy [29]. On the other hand, it is difficult to dilute the solid samples in
79 order to reduce IFE in SPF spectroscopy. Therefore, Lagorio et al. (1998) [30] has proposed a
80 correction factor via the modification of the Kubelka–Munk (KM) theory of diffuse reflectance,
81 and some studies have applied this correction [26,27].
82 However, a quantitative relationship between fluorescence intensity and organic matter
83 concentration was not observed by the application of this correction method to the SPF-EEM of
84 soil samples darkened by organic carbon or a black pigment [24]. This result possibly suggests
85 that additional correction methods and theoretical studies are required for dark solid samples. At

least, for the further utilization of SPF-EEM spectroscopy in the field, it is crucial to develop a practical method for quantifying the concentration of fluorescent species in solid samples from their solid-phase fluorescence spectra even when samples are affected by IFE.

In this study, the absorption and scattering of excitation light was assumed to considerably affect IFE in SPF-EEM spectroscopy, and a new parameter in terms of fluorescence intensity and diffuse reflection was proposed to quantify the fluorophore concentration. For this purpose, mixture powders simulating fluorescent sample with IFE were measured by an ultraviolet–visible (UV–Vis) spectrometer with an integrating sphere to obtain diffuse reflection spectra, as well as by a fluorescence spectrometer to obtain SPF-EEM spectra. Bovine serum albumin (BSA) and commercial pigments were selected as fluorescent and absorbing materials, respectively. It is assumed that the fluorescence of protein BSA is due to phenylalanine, tyrosine, and tryptophan. Among these amino acids, less amino acids are exposed outside the three dimensional structure than are incorporated inside the structure. Therefore, quenching effect due to interaction with other BSA particles and/or the absorbing materials is not considered in this study.

To perform these two analyses, it is crucial to prepare UV–Vis and fluorescence spectrometers and repack the sample or prepare a new cell commonly used in the two instruments. This is time-consuming and expensive, leading to a narrowed applicability in the field. Therefore, substitute spectra for diffuse reflection spectra are additionally examined by the Rayleigh scattering in 3D-EEM spectra without using a UV–Vis spectrometer, and the parameter is applied.

Materials and Methods

Sample Preparation

Bovine serum albumin was purchased from Wako, Japan (9048-46-8, specification assay: 98+%). The simulated diluent, boric acid (white powder) (Wako, Japan, 10043-35-3, purity: 99.5+%), was used referring to the previous research [19]. Commercial activated carbon powder (Wako, Japan, 7440-44-0) was used as a black colorant. These diluent powders were crushed in an agate mortar and sieved through a 63 μm mesh. The passed through was used for sample preparation. The other colorants, cinnabar (red, 10 μm particle size; Iwashinsha, 721, Nakagawa Gofun Enogu, Japan), azurite (blue, 14 μm particle size; Iwagunjo, 731, Nakagawa Gofun Enogu, Japan), and malachite (green, 10 μm particle size; Matsubarokusyo, 741, Nakagawa Gofun Enogu, Japan) powders, were used. A brown colorant was obtained by mixing 70 vol% red + 30 vol% green colorants. A purple colorant included a mixture of 70 vol% red + 30 vol% blue colorants. In preliminary measurements, these colorants did not exhibit any characteristic fluorescence.

For "colorant-concentration-fixed" measurements, 1, 5, 10, 20, 50, and 95 vol% BSA powders were prepared by mixing BSA and boric acid with and without the 5 vol% red/black colorant in the agate mortar for 10 min. To check a characteristic fluorescence pattern of BSA, 0 vol% BSA powders (powders of 100% boric acid, 100% red colorant, and 100% black colorant) and a 100 vol% BSA powder were also prepared.

On the other hand, 5 vol% BSA powders were obtained by mixing BSA, boric acid powder, and black, red, blue, green, brown, and purple colorants in the agate mortar for greater than 5 min, as shown in Supplementary Table s1. These samples were used for "BSA-concentration-fixed" measurements. Notably, the powders were mixed on the basis of the mass ratio determined from the desired volume concentration and densities.

Colorant-Concentration-Fixed Measurements

All SPF-EEM spectra were recorded using a fluorescence spectrophotometer (F-7100, Hitachi, Japan) with a sample stage (5J0-0133, Hitachi, Japan), which is designed so that the sample surface is tilted by 10° with respect to the plane composed of incident and detected light. The powder samples were sealed in an original plate-shaped quartz cell with internal dimensions of 19 mm width, 1 mm depth, and 19 mm height, which was constructed by Sansyo, Japan. The incident light was applied to the sample surface (the widest side) at an angle of 30°, and the emitted fluorescence was collected at an angle of 60°. The excitation wavelength (Ex.) ranged from 250 to 550 nm at 5 nm intervals (excitation slit: 2.5 nm bandpass), and the emission wavelength (Em.) ranged from 290 to 600 nm at 1 nm intervals (emission slit: 2.5 nm bandpass). The scanning speed was 30000 nm min^{-1}, and the photomultiplier voltage was 400 V. To remove second-order Rayleigh scattering, a filter with a cut-off wavelength of 290 nm was attached to the emission light pass.

Diffuse reflectance spectra were obtained using a UV–Vis spectrometer (U-3900, Hitachi, Japan) with an integrating sphere (2J2-0171, Hitachi, Japan) by using the original sample holder before fluorescence measurements. These measurements were conducted at a scanning speed of 300 nm min^{-1} with a 2 nm slit width in the 250–600 nm spectral range at a 0.5 nm interval. As a reference for calculating the reflectance [R_λ: λ is the wavelength] of the samples, a standard alumina (Al_2O_3) plate was used. R_λ was converted to the KM function (KM_λ) according to previous studies [24,31,32]. The KM spectrum represents the absorption spectrum of the powder sample, which is calculated by the following equation:

$$KM_\lambda = \frac{(1-R_\lambda)^2}{2R_\lambda} \qquad \text{Eq. 1}$$

The correction based on the KM theory [26,27,30] was conducted on fluorescence intensities by dividing by $\gamma(\lambda_0, \lambda_1)$:

$$\gamma(\lambda_0, \lambda_1) = \left(\frac{1}{1 + \sqrt{\frac{KM_{\lambda_1}}{KM_{\lambda_1} + 2}}} \right) \times \left(\frac{1}{1 + \sqrt{\frac{KM_{\lambda_1}(KM_{\lambda_1} + 2)}{KM_{\lambda_0}(KM_{\lambda_0} + 2)}}} \right) \quad \text{Eq. 2}$$

where λ_0 and λ_1 represent values of the excitation and emission wavelength, respectively.

BSA-Concentration-Fixed Measurements

For SPF-EEM spectral measurements, the measurement condition employed was almost the same as that utilized for colorant-concentration-fixed measurements, except for the use of a commercial sample holder (5J0-0133, Hitachi, Japan), slit conditions, and number of measurements. A cylindrical sample holder with a diameter of 12 mm was used, and the samples were sealed with a quartz window. A 5 nm bandpass excitation/emission slit was used.

Diffuse reflectance spectra were recorded using the UV–Vis spectrometer, and the original quartz cell under the same measurement condition as that utilized for colorant-concentration-fixed measurements was used. Therefore, the samples are reinjected to different holders after fluorescence measurements.

Results

Colorant-Concentration-Fixed Measurements

Fig.1 and Supplementary Fig. s1 show the three-dimensional (3D) SPF-EEM spectra of BSA, boric acid, the red colorant, and the black colorant. In the BSA spectrum (Fig. 1), two peaks at Ex. 280 nm/Em. 330 nm by BSA and Ex. 350 nm/Em. 422 nm possibly due to impurities were observed. In this study, the former peak was focused because of a more prominent signal. The

samples without BSA did not exhibit a significant fluorescence pattern at Ex. 280 nm/Em. 330 nm (BSA) [Figs. s1(a)–(c)].

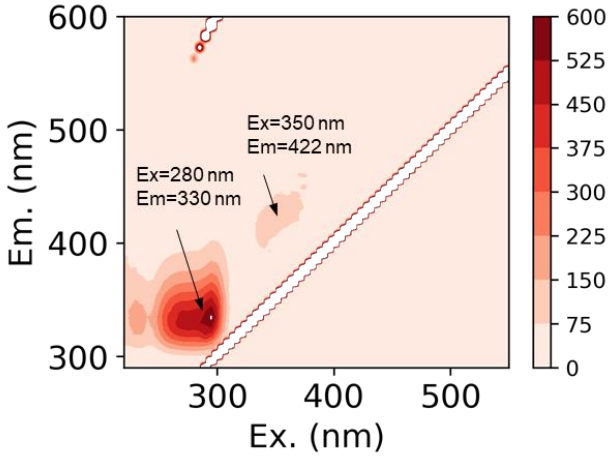


Figure 1. SPF-EEM spectra of BSA powder. Ex.: Excitation wavelength in nm; Em.: Emission wavelength in nm.

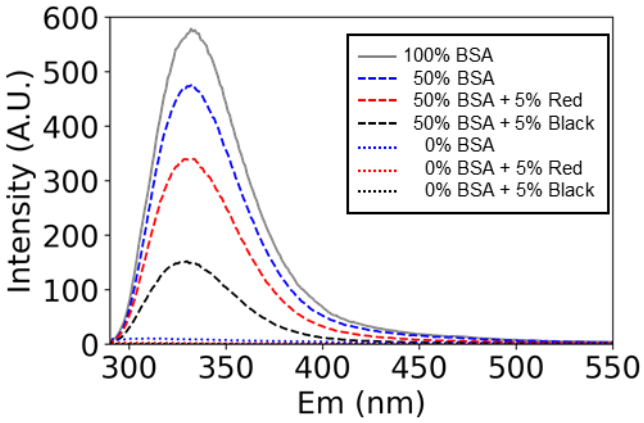


Figure 2. Representative emission spectra by the 280 nm excitation of BSA powder, boric acid, the red colorant, the black colorant, and their mixtures.

Emission spectra at Ex. 280 nm were extracted from all of the EEM spectra. Fig. 2 shows representative emission spectra of 0, 50, and 100 vol% BSA powders. The spectra of 0 vol% BSA

powder did not exhibit any significant fluorescence, and those of the other powders exhibited BSA-related fluorescence. The magnitude of the fluorescence intensity was in decreasing order of 100 vol% BSA, 50 vol% BSA + 50 vol% boric acid (white powder), 50 vol% BSA + 45 vol% boric acid + 5 vol% red colorant, and 50 vol% BSA + 45 vol% boric acid + 5 vol% black colorant, indicating that BSA concentration and colors of quenching media determine the detected fluorescence intensity [19,24].

Fig. 3(a) shows the fluorescence intensities at Ex. 280 nm/Em. 330 nm (Em_{330}) against the BSA concentration (vol%) of 1–95 vol% BSA samples and those with 5 vol% red/black colorants for clear comparison. BSA concentration in vol% can be converted to that in wt%. Fig. 3(b) shows the intensities Em_{330} against the BSA concentration (wt%). We identified different trends for the different colorants, which can be fitted by saturation curves:

$$Em_{330-cor} = A(1 - e^{-BC}) \qquad \text{Eq. 3}$$

where A and B are constants, and C is the BSA concentration. The fitted curves exhibited good reproducibility (Fig. 3).

In addition, the corrected fluorescence intensities at Ex. 280 nm/Em. 330 nm ($Em_{330\text{-cor}}$) were obtained by $\gamma(\lambda_{280}, \lambda_{330})$ (Eq. 2), including KM_{280} and KM_{330} [Supplementary Figs. s2(a) and (b)]. The KM functions were calculated by Eq. 1, using diffuse reflectance spectra of the 1–95 vol% BSA samples. Figs. 3(c) and (d) show $Em_{330\text{-cor}}$ against the BSA concentration in vol% and wt%, respectively. They exhibited trends almost similar to those of Em_{330} against the BSA concentration [Figs. 3(a) and (b)].

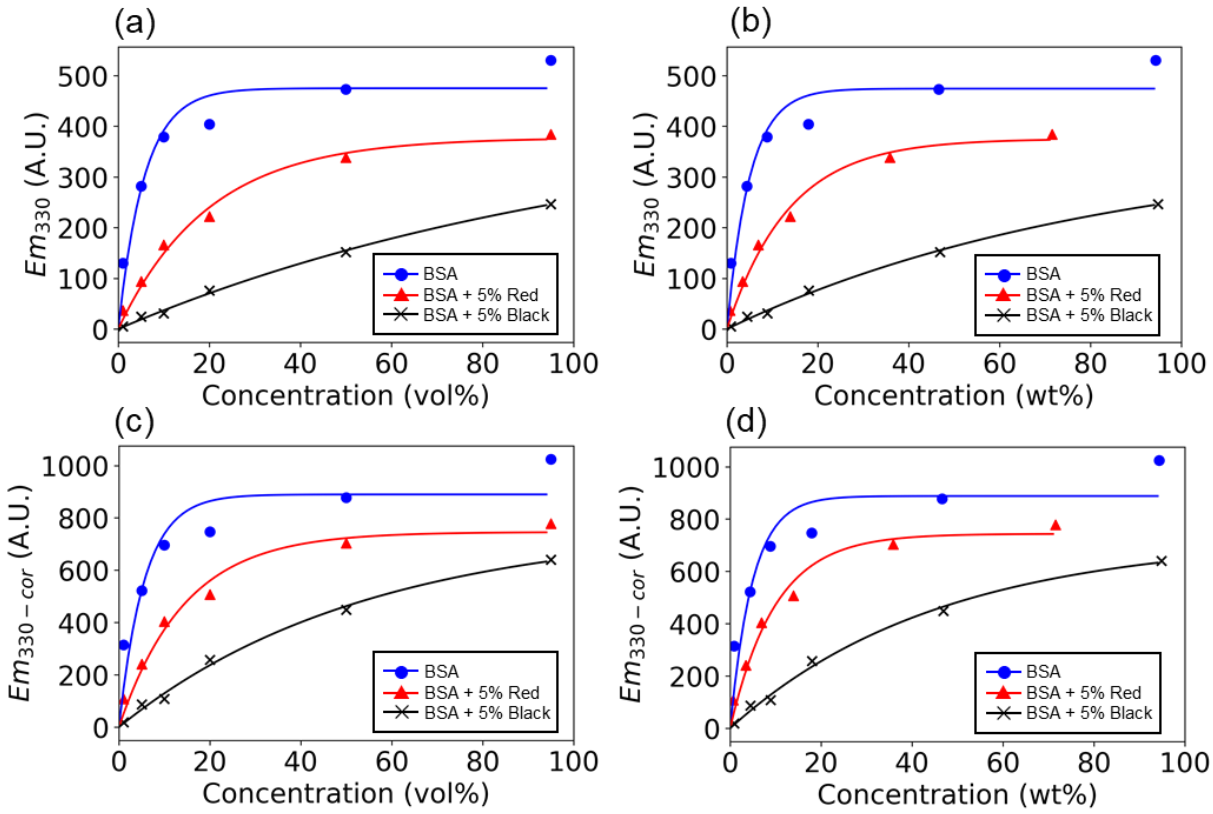


Figure 3. Raw fluorescence intensities at Ex. 280 nm/Em. 330 nm (Em_{330}) against the BSA concentration in (a) vol% and (b) wt% of 1–95 vol% BSA samples and those with 5 vol% red/black colorants. Corrected ones ($Em_{330\text{-cor}}$) against the BSA concentration in (c) vol% and (d) wt%. Solid curves represent the curves fitted by Eq. 3. Constants and decision coefficient r^2 values obtained from the fitting by Eq. 3 are shown in Supplementary Table s2.

BSA-Concentration-Fixed Measurements

By BSA-concentration-fixed measurements, values of Em_{330}, KM_{280}, and KM_{330} for 5 vol% BSA powders with various colorants were measured, and $Em_{330\text{-cor}}$ values were obtained by the KM-theory-based correction (Supplementary Table s1). Notably, fluorescence intensities of "BSA-concentration-fixed" measurements were generally greater than those of the "colorant-

concentration-fixed" measurements (Figs. 1–3), possibly because of the different measurement conditions of the slit width and/or sample holders.

The corrected intensities $EM_{330\text{-}cor}$ against KM_{280} and KM_{330} [Figs. 4(a) and (b)], as well as raw intensities EM_{330} (Supplementary Fig. s3), reveal that the fluorescence intensities exhibit inverse-proportional-like relationships to the adsorption degrees (KM functions) at the excitation and emission wavelengths. In other words, the absorption of excitation and emission light was considered to negatively affect the fluorescence intensity.

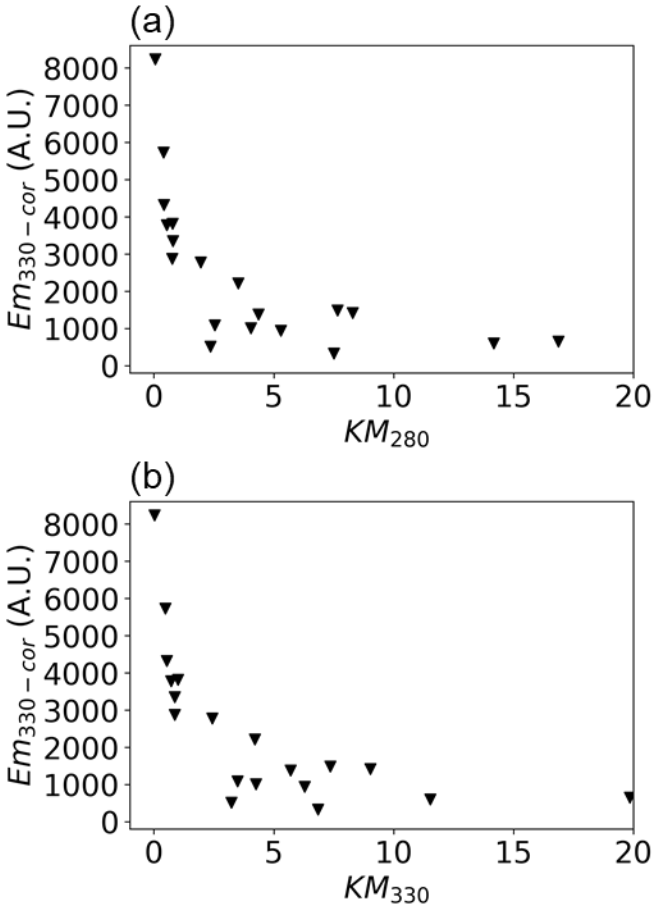
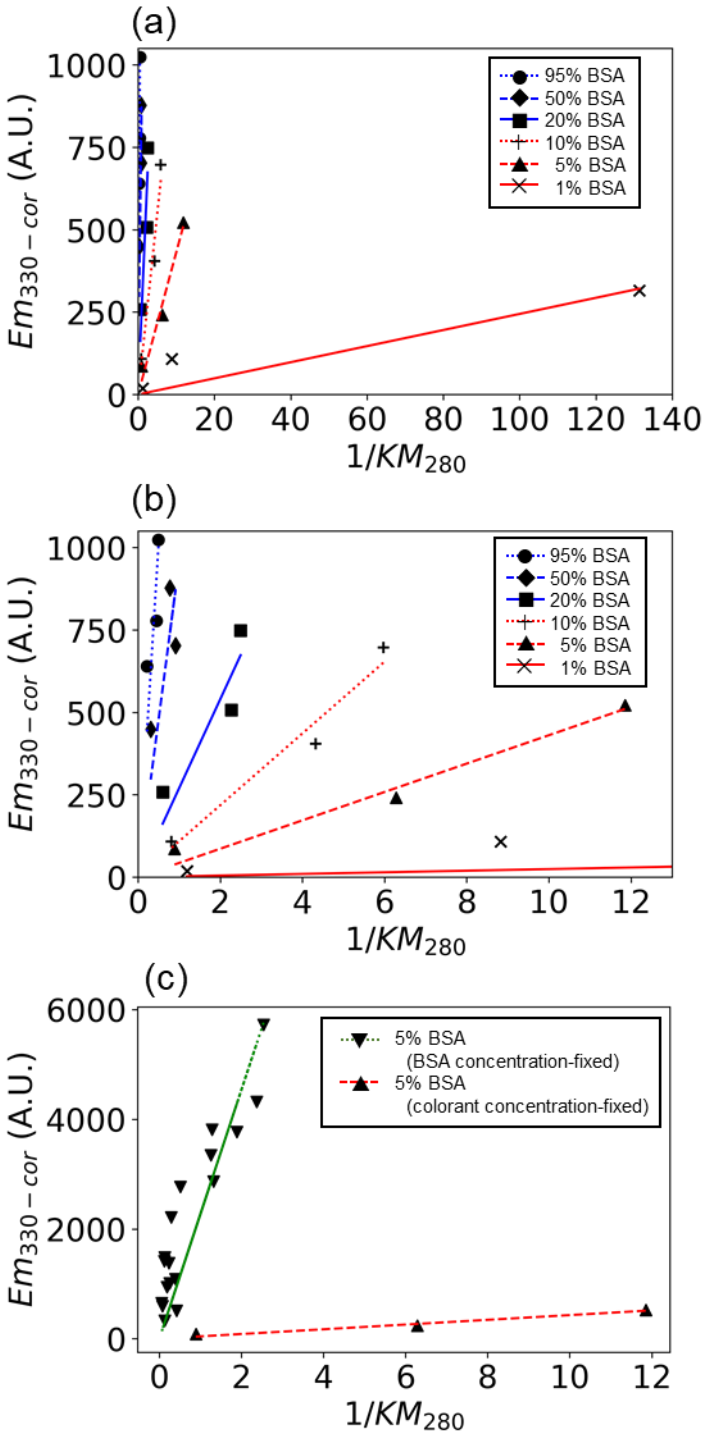


Figure 4. Corrected fluorescence intensities at Ex. 280 nm/Em. 330 nm ($Em_{330\text{-}cor}$) against KM functions at the (a) excitation wavelength (KM_{280}) and (b) emission wavelength (KM_{330}) of 5 vol% BSA with boric acid + various colorants (Supplementary Table s1).

Therefore, Figs. 5(a) and (b) shows the relationship between $EM_{330\text{-}cor}$ and $1/KM_{280}$ for 1–95 vol% BSA samples in the "colorant-concentration-fixed" measurements using the red and black colorants. And those in the "BSA concentration-fixed" measurements using the various colorants are also shown in Fig. 5(c). Different inversely proportional relationships at different BSA concentrations were observed. When data points for the white, red and black powders at the same BSA concentration were approximated by a straight line, the slope (constant of inverse proportion) increased with the increase in the BSA concentration. Notably, 5 vol% BSA samples for "colorant concentration-fixed" and "BSA concentration-fixed" measurements indicated different trend to each other [Fig. 5(c)], possibly due to the different measurement conditions in slit width and/or the sample holders. Relationships between $EM_{330\text{-}cor}$ and $1/KM_{330}$, EM_{330} and $1/KM_{280}$, and EM_{330} and $1/KM_{330}$ (Supplementary Fig. s4) also exhibited inverse-proportional-like trends, except for some data points where the KM function was large. Therefore, we made the hypothesis that the product of *EM* and *KM* exhibits a value specific to the BSA concentration even if *KM* varies, as long as the measurement conditions are the same. In this discussion chapter, a calibration curve for the BSA concentration was examined by the white, red and black samples (5 vol% colorants) with various KM values, assuming the BSA concentration dependence of the inverse proportionality constant between fluorescence intensities and KM functions.



242

243 **Figure 5.** Fluorescence intensities at Ex. 280 nm/Em. 330 nm (Em_{330}) against reciprocals of the

244 KM function at 280 nm ($1/KM_{280}$) of 1–95 vol% BSA samples in (a) $0 < 1/KM_{280} < 140$, (b) $0 <$

245 $1/KM_{280} < 12$ ranges, and (c) $0 < 1/KM_{280} < 12$ (for comparison of 5 vol% BSA samples in BSA

concentration-fixed and colorant concentration-fixed experiments) ranges. Colored lines are approximate straight lines for each concentration. Slopes approximated by the straight lines and decision coefficient r^2 values are shown in Supplementary Table s2.

Discussion

Novel Parameter for the Quantification of Fluorophores in Absorbing Media by SPF-EEM Spectroscopy

In principle, fluorescence intensity (Em_{λ_1}) under the excitation (λ_0) and emission (λ_1) wavelengths is expressed as the product of the intensity of the excitation light absorbed by the fluorescent species ($I_{\lambda 0\text{-absorbed}}$) and the apparent fluorescence quantum yield (Φ):

$$Em_{\lambda_1} = \Phi I_{\lambda_{0-absorbed}} \qquad \text{Eq. 4}$$

Φ can include the absolute quantum efficiency and the probability of fluorescence generation and experimental factors [19]. According to the Lambert–Beer law, $I_{\lambda 0\text{-absorbed}}$ is expressed as follows:

$$I_{\lambda_{0-absorbed}} = I_{\lambda_0}(1 - e^{-\varepsilon cl}) \qquad \text{Eq. 5}$$

where $I_{\lambda 0}$ is the incident intensity, ε is the absorption coefficient, c is the molecule content of absorbing species, and l is the pass length. Previously, Mounier et al. (2017) [19] have assumed that emissions are detected from the powdered sample surface by SPF-EEM measurements and suggested that the SPF intensity could be modeled by the following functional form:

$$Em_{\lambda_1} = \Phi I_{\lambda_0}(1 - e^{-\varepsilon cl}) \qquad \text{Eq. 6}$$

This result indicates that with the increase in c, the fluorescence intensity is saturated. Mounier et al. (2017) [19] have reported that the concentration dependence of the fluorescence of tryptophan and quinine sulfate in white powder (boric acid) can be well reproduced by Eq. 6. Similar results

have been obtained for the fluorescence of BSA diluted with sodium carbonate [15], and NOM in solid soil diluted with white powder [24].

In this study, the fluorescence of BSA also increased and was saturated with respect to the BSA concentration (Fig. 3), and it was well reproduced by Eq. 3, which exhibited a functional form similar to that shown in Eq. 6. However, differences between the saturation curves (Fig. 3) suggest that it is difficult to determine unknown BSA concentrations from fluorescence intensity in the presence of various quenching materials in a sample because one cannot obtain a single calibration curve that does not depend on the quenching medium in which the materials are mixed.

In fact, with the increase in the BSA concentration, KM_{280} [Supplementary Fig. s2(a)] increased because the adsorption center wavelength of BSA is 280 nm. The BSA in this study and in previous studies [19,24] are similar in that with the increase in the number of fluorescent species, the excitation light absorption increases. Therefore, the BSA fluorescence intensity can be modeled with the saturation curve (Eq. 3), which is similar to that reported in the previous studies (Eq. 6). However, KM_{280} also apparently reflected the effect of the colorants [Supplementary Fig. s2(a)], which possibly led to differences between the saturation curves (Fig. 3). Therefore, in analyzing actual natural samples containing various fluorescent and quenching species by UV–Vis and fluorescence spectroscopy, it may be not practical to calculate the contribution of fluorescent and absorbing species from the KM function at the excitation wavelength. In addition, it is impossible to physically separate the fluorescent and absorbing species. Therefore, a theoretical or an empirical formula is required to correct the fluorescence intensity to a parameter that is proportional only to the concentration of the fluorescent species, excluding the effect of absorbing substances. In this study, we observed an inverse-proportional-like relationship between the fluorescence intensities and KM functions for samples with 5 vol% BSA (Figs. 4 and s3). The

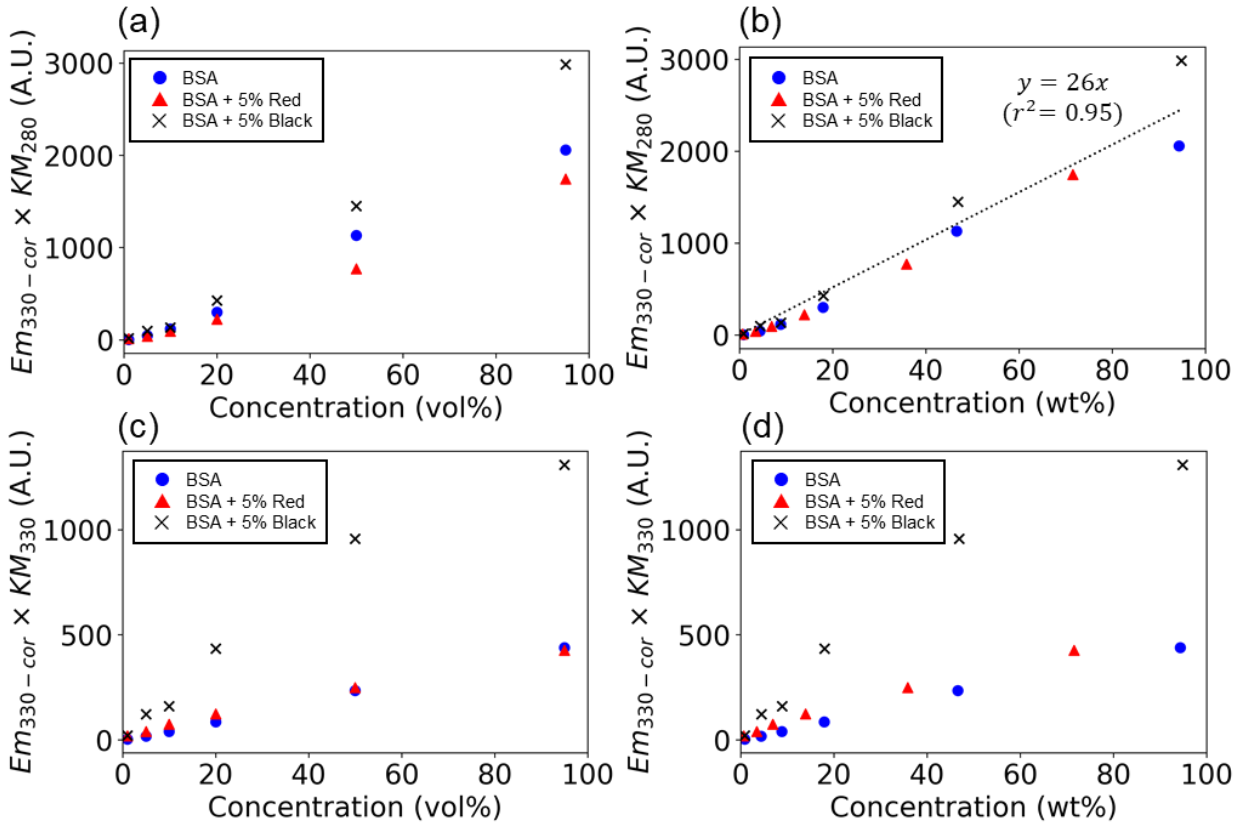
inversely proportional trend was specific to each BSA volume concentration (Fig. 5). As products of two inversely proportional parameters (in this case, $Em_{330\text{-}cor} \times KM_{280}$, etc.) can be constant, the empirical correction such as $Em_{330\text{-}cor} \times KM_{280}$, $Em_{330\text{-}cor} \times KM_{330}$, $Em_{330} \times KM_{280}$, and $Em_{330} \times KM_{330}$ was investigated to check whether it could correspond to the volume concentration of BSA.

Fig. 6(a) shows the values of $Em_{330\text{-}cor} \times KM_{280}$ plotted against the volume concentration of BSA. A linear trend reproducing their relationship was observed. On the other hand, Fig. 6(b) shows $Em_{330\text{-}cor} \times KM_{280}$ plotted against the "weight" concentration of BSA, indicative of a clearer single trend. The trend revealed a shape similar to that of a linear function. As the density of each absorbing colorant was different, the absolute amount of BSA and colorants differed in each colorant, even if the volume concentration of BSA was the same in the sample. Therefore, $Em_{330\text{-}cor} \times KM_{280}$ can be suggested as a parameter for the quantitative estimation of the unknown BSA "weight" concentration from SPF-EEM and UV–Vis spectroscopy of the BSA mixture powder.

Alternatively, a clear single trend was not recognized in $Em_{330\text{-}cor} \times KM_{330}$ plotted against the BSA concentration [Figs. 6(c) and (d)], where KM_{330} is the KM function at the "emission" wavelength. In black samples, the multiplication of KM_{330} over-corrected the fluorescence intensity extinction. That is, we could correct the fluorescence intensity to a parameter proportional to the BSA concentration by the multiplication with the KM function at the "excitation" wavelength, while the KM function at the "emission" wavelength led to the over-correction of the dark samples. This result suggests that the reabsorption of emission light may not contribute significantly to IFE due to dark materials. In other words, marginal fluorescence was generated inside the sample and transmitted through the sample to the detector. Therefore, we make the hypothesis that almost all of the observed fluorescence is emitted on the powder sample surface, and that components absorbing the excitation light prevent the excitation of fluorescent species.

This result was consistent with the assumption reported by Mounier et al. (2017) [19] that fluorescence is emitted only from the top surface of the sample.

On the other hand, results similar to the above discussion for the corrected intensities $Em_{330\text{-cor}}$ [Figs. 6(a)–(d)] were obtained for the raw intensities Em_{330} [Supplementary Figs. s5(a)–(d)], indicating that the KM-theory-based correction [26,27,30] does not significantly affect the quantification of BSA in absorbing media by the SPF method. In fact, this correction could not compensate for differences in the mixed colorants in this study [Figs. 3(c) and (d)], while the correction by KM_{280} multiplication provided the common calibration curve that was independent of colorant differences [Supplementary Figs. s5(a) and (b)]. The KM theory-based correction assumes that light emitted by the "primary" excitation of incident light can be absorbed and/or scattered within the sample or it can excite other fluorescent species, causing another "secondary" emission light. Therefore, the marginal effect by the KM-theory-based correction can be explained by the hypothesis that there is marginal fluorescence emitted from the inside of the sample. This indicates that the effect of absorption of the excitation (incident) light renders a large effect on fluorescence extinction in our BSA–colorant system.



329

330 **Figure 6.** Products of the corrected fluorescence intensities at Ex. 280 nm/Em. 330 nm and the
331 KM functions at 280 nm ($Em_{330\text{-cor}} \times KM_{280}$) against BSA concentration in (a) vol% and (b) wt%
332 of 1–95 vol% BSA. A dotted line in (b) is an approximate straight line. The function expression is
333 near the line, where x is the BSA concentration in wt%, y is $Em_{330\text{-cor}} \times KM_{280}$, and r^2 is a decision
334 coefficient. (c) and (d) represent products of the corrected fluorescence intensities at Ex. 280
335 nm/Em. 330 nm and the KM functions at "330 nm" ($Em_{330\text{-cor}} \times KM_{330}$) against BSA concentration
336 in vol% and wt%, respectively.

Use of Rayleigh Scattering on SPF-EEM Spectra as an Alternative to Diffuse Reflection Spectral Measurements by UV–Vis Spectrometer

To reduce the time and equipment cost of the UV–Vis spectrometer in the integrating-sphere measurement mode, diffuse reflection spectra were recorded by using the Rayleigh scattered light of the SPF-EEM spectra as substitutes. As a common reference spectrum, the Rayleigh scattered light of an SPF-EEM spectrum of the alumina plate was measured under the same measurement condition as that utilized for colorant-concentration-fixed measurements. Then, reflectance spectra were calculated by the Rayleigh scattered light signal of the samples (1–95 wt% BSA) and the reference, and their KM spectra were recorded. However, because the reference signal was saturated in the region at greater than 290 nm, KM functions were not appropriate except for the region at less than 290 nm, where the emission light was attenuated by the filter for removing second-order Rayleigh scattering. Therefore, SPF-EEM spectra of the samples and reference are recorded again at a photomultiplier voltage of 250 V. This resulted in appropriate KM spectra in the entire wavelength range, but fluorescence patterns were not detected probably because of the low detector sensitivity at 250 V. Supplementary Fig. s6 shows the comparison of representative KM spectra of 95 vol% BSA + 5 vol% boric acid from the UV–Vis spectrometer and the fluorescence spectrophotometer at photomultiplier voltages of 250 and 400 V.

Supplementary Figs. s7(a) and (b) show the KM functions at 280 and 330 nm of the samples by Rayleigh scattering measurements at a photomultiplier voltage of 250 V ($KM_{280\text{-R}}$ and $KM_{330\text{-R}}$: "-R" denotes that these parameters are obtained by the Rayleigh scattering measurements). The relationship between $KM_{280\text{-R}}$ or $KM_{330\text{-R}}$ and the BSA concentration was slightly different from KM_{280} or KM_{330} obtained with the UV–Vis spectrometer [Supplementary Figs. s2(a) and (b)]. This result is possibly attributed to the detection sensitivity of the Rayleigh scattering in SPF-EEM

spectroscopy. In addition, $Em_{330\text{-}cor\text{-}R}$ by γ(330, 280) using $KM_{280\text{-}R}$ and $KM_{330\text{-}R}$ was obtained. Values of $Em_{330\text{-}cor\text{-}R} \times KM_{280\text{-}R}$ against BSA weight concentrations then exhibited a single trend (Fig. 7). However, a clear correspondence to the BSA concentration was observed only in the region at greater than 40 wt%. Moreover, a single calibration curve of $Em_{330} \times KM_{280\text{-}R}$ (without the KM-theory-based correction) against BSA weight concentrations cannot be recognized although measurements by the fluorescence spectrometer and the UV–Vis spectrometer yielded calibration curves with and without the KM- theory-based correction. This result is possibly related to the fact that the KM functions used for the correction are not quantitative when they are obtained from Rayleigh scattering.

Although the above problems remain to be solved, the present results suggest that in the range of appropriate KM functions, we can obtain the novel parameter $Em_{\lambda 1} \times KM_{\lambda 0}$, which permits the quantification of the fluorescent species concentration by using only one fluorescence spectrophotometer. Notably, for preventing the saturation of the Rayleigh scattering signal, KM spectral measurements at a lower photomultiplier voltage or use of a mesh filter in front of the detector are required to reduce the light intensity before or after an EEM pattern measurement at a higher photomultiplier voltage for sufficient detection sensitivity. To address these problems, further application studies on other fluorophores and absorbing media must be conducted.

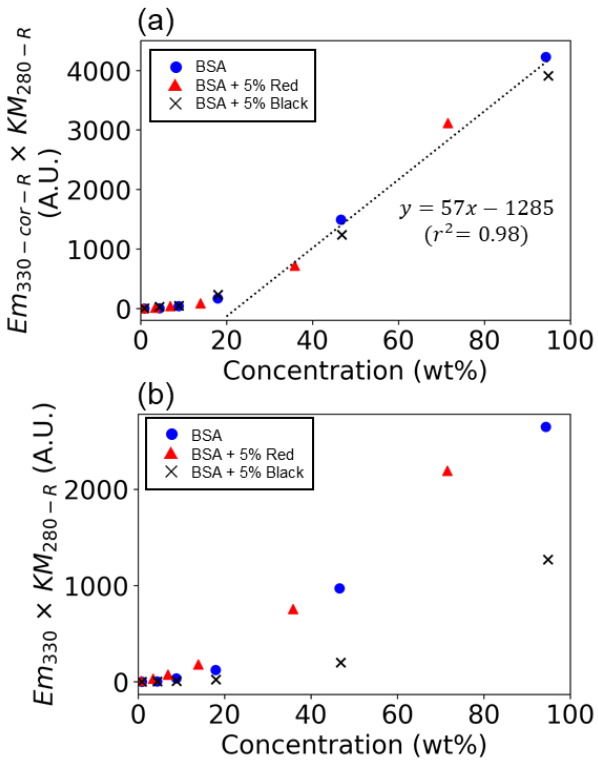


Figure 7. (a) Products of the corrected fluorescence intensities at Ex. 280 nm/Em. 330 nm and the KM functions at 280 nm obtained by Rayleigh scattering measurements at a photomultiplier voltage of 250 V ($Em_{330\text{-cor-R}} \times KM_{280\text{-R}}$) against BSA concentration (wt%) of 1–95 vol% BSA. The dotted curve represents an approximate curve with quadratic functions. The function expression is near the line, where x is the BSA concentration in wt%, y is $Em_{330\text{-cor-R}} \times KM_{280\text{-R}}$, and r^2 is a decision coefficient. (b) Products of the raw fluorescence intensities at Ex. 280 nm/Em. 330 nm and the KM functions at 280 nm obtained by Rayleigh scattering measurements at a photomultiplier voltage of 250 V ($Em_{330} \times KM_{280\text{-R}}$) against the BSA concentration (wt%).

Future Perspective

In this study, the products of fluorescence intensity obtained by SPF-EEM spectroscopy of the BSA-containing powder and its KM function at the excitation wavelength exhibit a specific trend

with respect to the BSA weight concentration. Moreover, this parameter was partially obtained by using the fluorescence spectrophotometer without using the UV–Vis spectrometer. By using this trend as an empirical calibration curve, SPF-EEM spectroscopy may be used for the quantification of BSA (a particular fluorescent material) mechanically mixed with white, red and black diluents (absorbing materials). In order to generalize this hypothesis, the authors are conducting further studies with other fluorescent and absorbing materials. Moreover, the authors did not consider fluorescence quenching due to interaction between fluorescent substances and other substances. Actual environmental samples include organic-mineral complexes and organic substances bound by supramolecular interactions.[33] This point should be considered for application of SPF to real environmental samples, especially heterogeneous environmental samples such as soil and sediment.

In future studies, empirical relationship between other materials more similar to samples in real environment should be examined. For example, NOM can be either fluorescent material and absorbing material. Yamamura et al. (2019) [21] have applied SPF-EEM spectroscopy as a non-destructive method for monitoring fouling organic substances in water-purifying membranes. According to their study, as potential fouling materials, hydrophilic (HPI: fluorescent/colorless), transphilic (TPI: fluorescent/colorless), and hydrophobic (HPO: non-fluorescent/yellowish) fractions in the powder state were extracted from natural water samples. Therefore, SPF-EEM spectroscopy is investigated in a system in which the fluorescence of HPI/TPI materials is absorbed by HPO materials in the powdered and filter-attached states. For these systems, the possibility of their quantification by $Em_{\lambda 1} \times KM_{\lambda 0}$ is also under investigation.

We are also studying an application of this study to correct an entire SPF-EEM spectrum so that its intensity increases linearly with the concentration of fluorescent species. As a result, it may be

possible to determine the contribution ratio of multiple fluorescence components from an SPF-EEM spectrum by applying peak separation such as EEM-PARAllel FACtor (EEM-PARAFAC) analysis, which is proposed in LPF-EEM spectroscopy [34, 35], to SPF-EEM spectroscopy. Moreover, the physical meaning of the trends should also be considered. Correspondence to those proportionality constants is not clear. Understanding the theoretical basis of this correspondence, as well as finding differences and similarities among various fluorescent species and absorbing media is crucial to successfully applying SPF-EEM spectroscopy for the analysis of solid-state NOM samples.

Conclusion

SPF-EEM spectroscopy of model mixtures of BSA and various colorants simulating fluorescent NOM samples was examined, and different saturation curves for fluorescence intensities against BSA concentrations for different colorants were observed. However, the KM-corrected fluorescent intensities (products of the fluorescence intensity and KM function at the excitation wavelength) were proportional to the first-order BSA weight concentration, regardless of the colorant type. This result possibly suggests that the absorption/scattering of the excitation light considerably affects fluorescence extinction in SPF spectroscopy. By using the trend as an empirical calibration curve, quantification of a particular fluorescent material from its SPF-EEM spectrum may be possible. Moreover, the KM functions are partially obtainable from the fluorescence spectrophotometer by use of the Rayleigh scattering in the SPF-EEM spectra, making the application of SPF-EEM spectroscopy in the field more convenient. Although the physical meaning of the parameters and the mechanism are still unclear, further studies are expected to

enhance the applicability of SPF-EEM spectroscopy for the quantitative and qualitative analysis of NOM.

Declaration of Competing interest

The authors declare that they have no known competing financial interests or personal relationships that could have appeared to influence the work reported in this paper.

Funding

This work was supported by JSPS Kakenhi Grant Numbers 20H02288 and 20K19958.

Supporting Information

There are three tables and six figures in the Supplementary Materials. The materials are available free of charge via the Internet (https://doi.org/10.1016/j.saa.2022.121885).

References

[1] Kördel, W., Dassenakis, M., Lintelmann, J. and Padberg, S. (1997) The importance of natural organic material for environmental processes in waters and soils. (Technical Report) *Pure Appl. Chem.*, 69, 1571–1600. DOI:10.1351/pac199769071571

[2] Zhang, Y., Zhao, X., Zhang, X. and Peng, S, (2015) A review of different drinking water treatments for natural organic matter removal. *Water Sci. Technol.: Water Supply.*, 15, 442–455. DOI: 10.2166/ws.2015.011

[3] Golea, D. M., Upton, A., Jarvis, P., Moore, G., Sutherland, S., Parsons, S. A. and Judd, S. J. (2017) THM and HAA formation from NOM in raw and treated surface waters. *Water Res.*, 112, 226–235. DOI: 10.1016/j.watres.2017.01.051

[4] Amy, G. (2008) Fundamental understanding of organic matter fouling of membranes. *Desalination*, 231, 44–51. DOI: 10.1016/j.desal.2007.11.037

[5] Aiken, G. R. (1985) Isolation and concentration techniques for aquatic humic substances, in: Aiken, G. R., McKnight, D. M., Wershaw, R. L. and MacCarthy, P. (Eds.), *Humic substances in soil, sediment and water: geochemistry and isolation*, Wiley-Interscience, pp. 363–385.

[6] Swift, R. S. (1996) Organic matter characterization, in: Sparks, D. L., Page, A. L., Helmke, P. A., Loeppert, R. H., Soltanpour, P. N., Tabatabai, M. A., Johnson, C. T. and Summer, M. E. (Eds.), *Methods of soil analysis. Part 3. Chemical methods*, Soil Science Society of America, 1018–1020.

[7] Lehmann, J. and Kleber, M. (2015) The contentious nature of soil organic matter. *Nature* 528, 60–68. DOI: 10.1038/nature16069

[8] Olk, D.C., Bloom, P. R., Perdue, E. M., Chen, Y., McKnight, D. M., Farenhorst, A., Senesi, N., Chin, Y. P., Schmitt-Koplin, P., Hertkorn, N. and Harir, M. (2019) Environmental and agricultural relevance of humic fractions extracted by alkali from soils and natural waters. *J. Environ. Qual.* 48, 217–232. DOI:10.2134/jeq2019.02.0041

[9] Kleber, M and Lehmann, J. (2019) Humic substances extracted by alkali are invalid proxies for the dynamics and functions of organic matter in terrestrial and aquatic ecosystems. *J. Environ. Qual.* 48, 207–216. DOI: 10.2134/jeq2019.01.0036

[10] Myneni, S. C. B. (2019) Chemistry of natural organic matter—The next step: commentary on a humic substances debate. *J. Environ. Qual.* 48, 233–235. DOI: 10.2134/jeq2019.02.0002c

[11] Yamamura, H., Okimoto, K., Kimura, K. and Watanabe, Y. (2014) Hydrophilic fraction of natural organic matter causing irreversible fouling of microfiltration and ultrafiltration membranes. *Water Res.* 54, 123–136. DOI: 10.1016/j.watres.2014.01.024

[12] Sheng, G. P., Yu, H.Q. and Li, X. Y. (2010) Extracellular Polymeric Substances (EPS) of microbial aggregates in biological wastewater treatment systems: a review. *Biotechnol. Adv.*, 28, 882–894. DOI: 10.1016/j.biotechadv.2010.08.001

[13] Senesi, G. S., Martin-Neto, L., Villas-Boas, P. R. Nicolodelli, G. Milori, D. M. B. P. (2018) Laser-based spectroscopic methods to evaluate the humification degree of soil organic matter in whole soils: a review. J. Soil Sediment. 18, 1292–1302. DOI: 10.1007/s11368-016-1539-6

[14] Milori, D.M.B.P., Galeti, H.V.A., Martin-Neto, L., Dieckow, J., González-Pérez, M., Bayer, C. and Salton, J. (2006) Organic matter study of whole soil samples using laser-induced fluorescence spectroscopy. *Soil Sci. Soc. Am. J.* 70, 57–63. DOI: 10.2136/sssaj2004.0270

[15] Muller, M., Milori, D. M. B. P., Déléris, S., Steyer, J. P. P. and Dudal, Y. (2011) Solid-phase fluorescence spectroscopy to characterize organic wastes. *Waste Management* 31, 1916–1923. DOI: 10.1016/j.wasman.2011.05.012

[16] Alves, J. C. L. and Poppi, R.J. (2013) Pharmaceutical analysis in solids using front face fluorescence spectroscopy and multivariate calibration with matrix correction by piecewise direct standardization. *Spectrochim. Acta A Mol. Biomol. Spectrosc.* 103, 311–318. DOI: 10.1016/j.saa.2012.10.074

[17] Ammari, F., Bendoula, R., Jouan-Rimbaud Bouveresse, D., Rutledge, D. N. and Roger, J. M. (2014) 3D front face solid phase fluorescence spectroscopy combined with Independent Components Analysis to characterize organic matter in model soils. *Talanta* 125, 146–152. DOI: 10.1016/j.talanta.2014.02.049

[18] Albrecht, R., Verrecchia, E. and Pfeifer, H. R. (2015) The use of solid-phase fluorescence spectroscopy in the characterisation of organic matter transformations. *Talanta* 134, 453–459. DOI: 10.1016/j.talanta.2014.11.056

[19] Mounier, S., Nicolodelli, G., Redon, R. and Milori, D. M. B. P. (2017) Direct solid surface fluorescence spectroscopy of standard chemicals and humic acid in ternary system. *Spectrochim. Acta A Mol. Biomol. Spectrosc.* 177, 79–85. DOI: 10.1016/j.saa.2017.01.017

[20] Guan, Y. F., Qian, C., Chen, W., Huang, B. C., Wang, Y. J. and Yu, H. Q. (2018) Interaction between humic acid and protein in membrane fouling process: a spectroscopic insight. *Water Res.*, 145, 146–152. DOI: 10.1016/j.watres.2018.08.019

[21] Yamamura, H., Ding, Q. and Watanabe, Y. (2019) Solid-phase fluorescence excitation emission matrix for in-situ monitoring of membrane fouling during microfiltration using a polyvinylidene fluoride hollow fiber membrane. *Water Res.*, 164, 114928. DOI: 10.1016/j.watres.2019.114928

[22] Yu, H., Wu, Z., Zhang, X., Qu, F., Wang, P. and Liang, H. (2019) Characterization of fluorescence foulants on ultrafiltration membrane using front-face excitation-emission matrix (FF-EEM) spectroscopy: fouling evolution and mechanism analysis. *Water Res.*, 148, 546–555. DOI: 10.1016/j.watres.2018.10.041

[23] Ding, Q., Ochiai, K. and Yamamura, H. (2020) In situ and online monitoring of the chemical cleaning efficiency by solid-phase fluorescence excitation–emission matrix spectroscopy (SPF-EEM). *J. Membr. Sci.*, 611. 118296. DOI: 10.1016/j.memsci.2020.118296

[24] Nakaya, Y., Nakashima, S., Moriizumi, M., Oguchi, M., Kashiwagi, S. and Naka, N. (2020) Three dimensional excitation-emission matrix fluorescence spectroscopy of typical Japanese

soil powders. *Spectrochim. Acta A Mol. Biomol. Spectrosc*. 233, 118188. DOI: 10.1016/j.saa.2020.118188

[25] Boughattas, F., Le Fur, B. and Karoui, R. (2019) Identification and quantification of tuna species in canned tunas with sunflower medium by means of a technique based on front face fluorescence spectroscopy (FFFS). *Food Control*, 101, 17–23. DOI: 10.1016/j.foodcont.2019.02.003

[26] Verri, G., Clementi, C., Comelli, D., Cather, S. and Piqué, F. (2008) Correction of ultraviolet-induced fluorescence spectra for the examination of polychromy. *Appl. Spectrosc.* 62, 1295–1302. DOI: 10.1366/000370208786822296

[27] Clementi, C., Miliani, C., Verri, G., Sotiropoulou, S., Romani, A., Brunetti, B. G. and Sgamellotti, A. (2009) Application of the Kubelka-Munk correction for self-absorption of fluorescence emission in carmine lake paint layers. *Appl. Spectrosc.* 63, 1323–1330. DOI: 10.1366/000370209790109058

[28] Lakowicz, J.R. (1999) *Principles of fluorescence spectroscopy*, Springer.

[29] Panigrahi, S. K. and Mishra, A. K. (2019), Inner filter effect in fluorescence spectroscopy: As a problem and as a solution. *J. Photochem. Photobiol. C: Photochem. Rev.*, 41, 100318, DOI:10.1016/j.jphotochemrev.2019.100318

[30] Lagorio, M. G., Dicelio, L. E., Litter, M. I. and San Román, E. (1998) Modeling of fluorescence quantum yields of supported dyes Aluminium carboxyphthalocyanine on cellulose. *J. Chem. Soc. Faraday Trans.* 94, 419–425. DOI: 10.1039/A706113G

[31] Onga, C. and Nakashima, S. (2014) Darkfield reflection visible microspectroscopy equipped with a color mapping system of a brown altered granite. *Appl. Spectrosc.* 68, 740–748. DOI: 10.1366/13-07255

[32] Okada, K. and Nakashima, S. (2019) Combined microspectroscopic characterization of a red-colored granite rock sample. *Appl. Spectrosc.* 73, 781–793. DOI: 10.1177/0003702818823555

[33] Ohno, T., Hess, N. J. and Qafoku, N. P. (2019) Current understanding of the use of alkaline extractions of soils to investigate soil organic matter and environmental processes. *J. Environ. Qual.* 48, 1561-1564.DOI: 10.2134/jeq2019.08.0292

[34] Murphy, K., Bro, R., and Stedmon, C. (2014) Chemometric Analysis of Organic Matter Fluorescence, in: Coble, P., Lead, J., Baker, A., Reynolds, D. and Spencer, R. (Eds.), *Aquatic Organic Matter Fluorescence*, Cambridge: Cambridge University Press. pp. 339–375. doi:10.1017/CBO9781139045452.016

[35] Wells, M. J. M., Hooper, J., Mullins, G. A., Bell, K. Y. (2022) Development of a fluorescence EEM-PARAFAC model for potable water reuse monitoring: Implications for inter-component protein-fulvic-humic interactions. *Sci. Total Environ.* 820, 153070. DOI: 10.1016/j.scitotenv.2022.153070